analytical chemistry

Subscriber access provided by UNIV AUTONOMA DE COAHUILA UADEC

Article

Ferritin-based Electrochemiluminescence Nanosurface Energy Transfer System for Procalcitonin Detection Using HWRGWVC Heptapeptide for Site-oriented Antibody Immobilization

Lei Yang, Dawei Fan, Yong Zhang, Caifeng Ding, Dan Wu, Qin Wei, and Huangxian Ju

Anal. Chem., **Just Accepted Manuscript** • Publication Date (Web): 10 May 2019

Downloaded from http://pubs.acs.org on May 10, 2019

Just Accepted

"Just Accepted" manuscripts have been peer-reviewed and accepted for publication. They are posted online prior to technical editing, formatting for publication and author proofing. The American Chemical Society provides "Just Accepted" as a service to the research community to expedite the dissemination of scientific material as soon as possible after acceptance. "Just Accepted" manuscripts appear in full in PDF format accompanied by an HTML abstract. "Just Accepted" manuscripts have been fully peer reviewed, but should not be considered the official version of record. They are citable by the Digital Object Identifier (DOI®). "Just Accepted" is an optional service offered to authors. Therefore, the "Just Accepted" Web site may not include all articles that will be published in the journal. After a manuscript is technically edited and formatted, it will be removed from the "Just Accepted" Web site and published as an ASAP article. Note that technical editing may introduce minor changes to the manuscript text and/or graphics which could affect content, and all legal disclaimers and ethical guidelines that apply to the journal pertain. ACS cannot be held responsible for errors or consequences arising from the use of information contained in these "Just Accepted" manuscripts.

ACS Publications

is published by the American Chemical Society. 1155 Sixteenth Street N.W., Washington, DC 20036

Published by American Chemical Society. Copyright © American Chemical Society. However, no copyright claim is made to original U.S. Government works, or works produced by employees of any Commonwealth realm Crown government in the course of their duties.

Ferritin-based Electrochemiluminescence Nanosurface Energy Transfer System for Procalcitonin Detection Using HWRGWVC Heptapeptide for Site-oriented Antibody Immobilization

Lei Yang,[†] Dawei Fan,[†] Yong Zhang,[†] Caifeng Ding,[‡] Dan Wu,[†] Qin Wei,[†,*] Huangxian Ju[†]

[†] Key Laboratory of Interfacial Reaction & Sensing Analysis in Universities of Shandong, School of Chemistry and Chemical Engineering, University of Jinan, Jinan 250022, PR China.

[‡] Key Laboratory of Optic-electric Sensing and Analytical Chemistry for Life Science, Ministry of Education, College of Chemistry and Molecular Engineering. Qingdao University of Science and Technology, Qingdao 266042, PR China.

ABSTRACT: In this study, an ultrasensitive biosensor based on a novel electrochemiluminescence nanosurface energy transfer (ECL-NSET) system was developed for procalcitonin (PCT) detection. *N*-(aminobutyl)-*N*(ethylisoluminol) (ABEI) as ECL donor was externally cross-linked with ferritin (ABEI-Ft), whose ECL emission was boosted by ferritin nanocore in the presence of hydrogen peroxide. Then, single gold nanoparticle (Au NP) as ECL acceptor was in situ reduced on ABEI-Ft surface to fabricate a donor-acceptor nanostructure (ABEI-Ft@Au). ECL quenching occurred in ABEI-Ft@Au correlates well with the NSET theory rather than Förster resonance energy transfer (FRET). To improve sensitivity of biosensor, HWRGWVC heptapeptide (HWR) was utilized to capture antibody Fc portion via specific interaction to realize site-oriented immobilization. After connecting with ABEI-Ft@Au via Au-S bond, HWR improved the incubation efficiency of antibody with a better maintained biological activity. Under optimal conditions, the proposed biosensor provided a quantitative readout to PCT concentration in the range of 100 fg/mL- 50 ng/mL with a detection limit of 41 fg/mL. With favorable specificity, stability and reproducibility, this highly efficient ECL-NSET system will inspire more interests in nanometal-based ECL quenching mechanism studies and developments of new methods for site-oriented antibody immobilization improve the sensitivity.

■ INTRODUCTION

Electrochemiluminescence (ECL), a light-emission progress generated from the excited luminous species, has received considerable attention due to high sensitivity, low background noises, wide dynamic response ranges and favorable controllability.[1-3] To date, ECL system based on energy transfer theory has become an uprising focus in bioanalysis, clinical diagnosis and pharmaceutical analysis.[4-7] Notably, gold nanoparticles (Au NPs) have been employed as energy acceptors to quench ECL emission of various luminophores.[8-10] However, some of the involved mechanisms still remain unspecified despite Förster resonance energy transfer (FRET) has been used to verify the quenching process,[7] thus making it essential to establish other qualified models to infer the possible mechanisms. As a nonradiative excitation energy transfer from molecular dipole to nanometal surface, nanometal surface energy transfer (NSET) is gaining growing attention in nanometer distance measurements, cell apoptosis monitoring and fluorescence quenching.[11-14] Recently, NSET has been utilized to reveal and demonstrate the quenching effects of nanometals toward fluorescence dyes.[15, 16] Though similar to FRET, NSET theory has not been applied to determine ECL quenching mechanisms and measure the distance between ECL donors and acceptors by now. Herein, concept of ECL-NSET is firstly brought up in this work, aiming at building a new quenching model for specific energy-transfer mechanism determinations between various ECL donors and nanometal-based ECL acceptors.

As well known, *N*-(aminobutyl)-*N*-(ethylisoluminol) (ABEI) with high and stable ECL efficiency can generate ECL signals with hydrogen peroxide (H_2O_2) as coreactant in alkaline solutions.[17] Due to the long steric distance between the primary amino group and benzene ring, ABEI exhibited favorable reducibility and has been used for in-situ preparation of Au NPs in ECL sensing systems.[17, 18] For improving the biocompatibility of biosensors, some nanosized biomaterials like DNA nanoscaffolds[13, 19] and protein nanocages[20], have been explored as ECL nanocarriers. Ferritin is a ubiquitous iron-storage protein which encapsulates a ferric nanocore within the nanocage composed of 24 subunits.[21, 22] With unique structural features, pH-tolerant property, biocompatibility, enzyme-mimic property, ferritin has been extensively utilized as nanoreactors for synthesis of nanomaterials, fabrication of nanodevices and controllable delivery of bioactive molecules, etc.[23-27] It should be highlighted that the ferric nanocore with enzyme-mimic activity can efficiently catalyze the oxidation of ECL luminophores in the presence of H_2O_2.[28] Inspired by this, ferritin as a natural, catalytic and biocompatible nanocarrier was served to crosslink with ABEI whose ECL emission will be boosted by the inside ferric nanocore.

It is worth noticing that the antigen-recognition ability of biosensor is mainly dominated by the biological activity of immobilized antibody.[29] Although abundant amino and hydroxyl groups are exposed on the outer surface of ferritin, random immobilization of antibodies via amine reaction can't guarantee their biological activity.[30] Due to the fact that $F(ab')_2$ fragment is the active section of antibody that interacts with antigen, when it fully or partially participates in the immobilization process, the antibody activity would decrease or even lost.[22] To avoid random immobilization and improve the availability of antibody for antigen binding, site-oriented immobilization is of great importance. To date, developments of small peptide ligands light up the way for

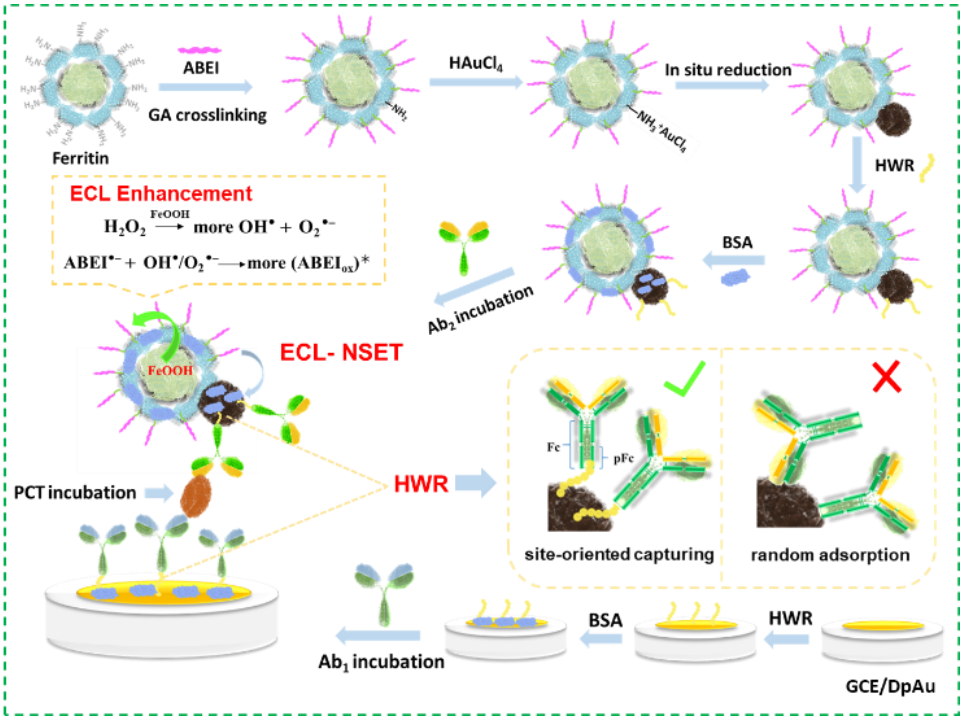

Scheme 1. The fabrication process of the proposed biosensor.

site-oriented antibody immobilization on nanocarriers.[29] In particular, HWRGWV hexapeptide has been demonstrated to specifically interact with the amino acids in the loop Ser383-Asn389 (SNGQPEN) of antibody Fc fragment with high affinity.[31] Possessing superiorities of low cost, easy preparation, physical and chemical stability, HWRGWV holds great potential in ECL immunoassay for site-oriented antibody immobilization.

In view of the above, a novel ECL biosensor was firstly proposed using ferritin-based ECL-NSET system with a new site-oriented antibody immobilization method. First of all, ABEI molecules were cross-linked on ferritin outer surface (ABEI-Ft) via glutaraldehyde (GA) interaction. $AuCl_4^-$ ions were adsorbed by amino groups of ferritin surface via electrostatic adsorption, which was then reduced to Au NPs (3.8 ± 0.2 nm) by proximal ABEI to form an donor-acceptor nanostructure of ABEI-Ft@Au. The quenching between proximal ABEI and Au NP correlated well with NSET theory by following a $1/d^4$ distance dependence. Then, the C-terminus of HWRGWV hexapeptide was modified with a cysteine to obtain HWRGWVC heptapeptide (HWR) which could combine with ABEI-Ft@Au via Au-S bond to specifically capture antibody in a site-oriented way.[20] Notably, HWR greatly accelerated the incubation of antibody with a better maintained activity, which saved a lot of time and improved the effective availability of antibody as well. Procalcitonin (PCT) as a reliable biomarker of systemic inflammatory response syndrome (SIRS) was employed as a target analyte.[32, 33] The developed biosensor based on ABEI-Ft@Au-HWR was constructed, which realized sensitive detection of PCT in human serums. This strategy will provide a new perspective for designing facile, biocompatible and eco-friendly ECL signal labels and quenching mechanism studies.

■ EXPERIMENTAL SECTION

Preparation of Ferritin and HWR Solution. Ferritin solution (100 mg/mL) was diluted to desired concentration of 10 ug/mL with 0.05 mol/L pH 7.4 phosphate buffer (PBS) that contained 0.05 mol/L NaCl. 1 mg of HWR was dispersed with 0.1 mol/L PBS (pH 7.4) and diluted to desired concentration of 1 ug/mL. Both ferritin and HWR solution were stored at 4 °C for further use. The preparation details of apoferritin (ferritin devoid of ferric nanocore) were shown in **Supporting Information** for the following enzyme-mimic activity study.

Preparation of ABEI-Ft@Au Nanostructure. First, 4 mL of ferritin (5 ug/mL), 1.5 mL of ABEI (10 mmol/L) solution were added into a 50 mL beaker, the mixture was then diluted with 4.5 mL of ultrapure water. After that, 100 µL of GA (50%) solution was added and kept stirring for 2 h to obtain the crosslinking product of ABEI-Ft. In the following step, 200 µL of $HAuCl_4$ (10 mmol/L) solution was injected into the above mixture for stirring 15 min. After that, the reaction was kept stirring at 50 °C for 5 min until the color changed from pale yellow to wine red. The ABEI-Ft@Au was centrifuged at 8000 rpm to discard excess reagents and then dispersed into 1 mL of ultrapure water .

Preparation of ABEI-Ft@Au-HWR-Ab_2 Bioconjugate. Then, 1 mL of HWR solution (50 ng/mL) was added into the above solution and the mixture was oscillated for 50 min at 4 °C. After centrifugation at 12000 rpm, the sediments were dispersed into 1 mL of PBS. Then, 400 uL of BSA solution (0.1%) was added to block the unspecific biding sites. After centrifugation and washing, 5 ug of Ab_2 was incubated at 4 °C for 40 min. After centrifugation and washing, the obtained ABEI-Ft@Au-HWR-Ab_2 bioconjugate was added into 1 mL of PBS (pH 7.4) for dispersion and then stored at 4 °C for further study.

High Performance Liquid Chromatography (HPLC) Analysis. Agilent 1260 HPLC system consisting of an UV detector and a Zorbax C18 column (4.6 ×250 mm, 5 µm) was utilized to conduct HPLC analysis in this work. Samples were eluted by the use of a mobile phase of acetonitrile/water (30:70, v/v). For the mobile phase, the injection volume of sample was 10 uL with a flow rate of 0.5 mL/min, and the wavelength was set to 220 nm. To assay the amounts of HWR that connected via Au-S bond, the centrifugation (8000 rpm for 10 min) supernatants of ABEI-Ft@Au-HWR bioconjugate were collected. Binding ratio (%) of HWR was calculated according to the following equation:

binding ratio (%) = connected HWR (ug)/ HWR (ug)× 100%

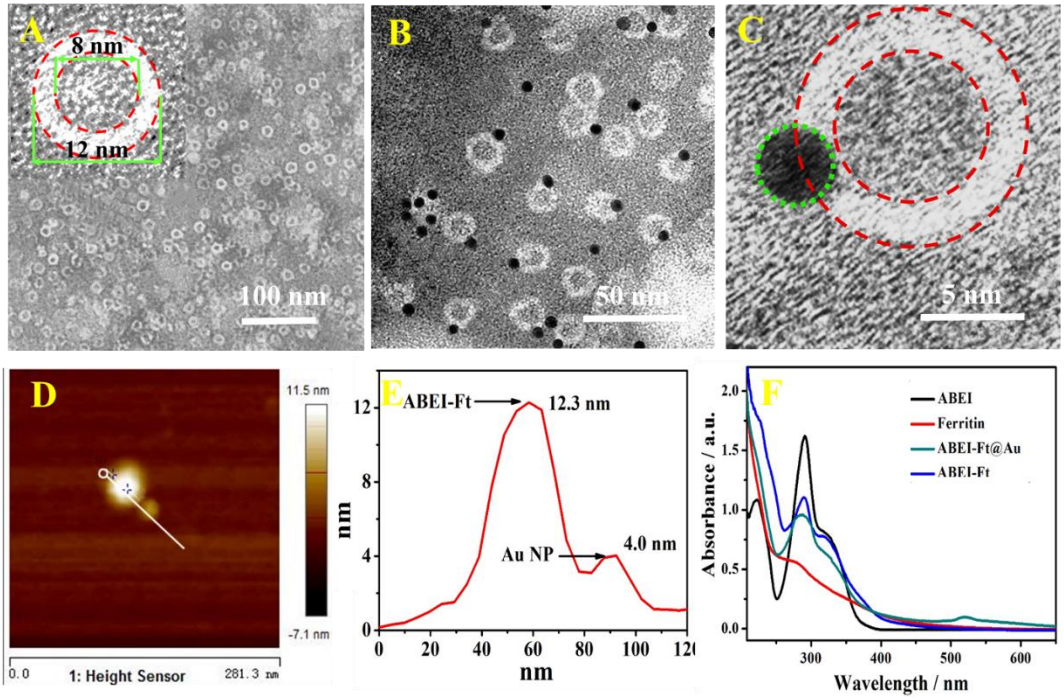

Figure 1. Negative stain TEM image of pure ferritin (A) and ABEI-Ft@Au (B), HRTEM image (C), all the samples were stained with 2% uranyl acetate for 3 min. AFM image (D) and height profile of single ABEI-Ft@Au nanostructure (E), UV-vis absorption spectrum of ABEI, ferritin, ABEI-Ft and ABEI-Ft@Au (F).

Circular Dichroism (CD) Analysis. CD spectroscopy is a powerful technique that sensitive to the secondary structural changes of protein or peptides when connected to substrate surfaces.[34] CD spectra was utilized to demonstrate the antibody activity after immobilizations through HWR specific interaction and Au-N adsorption, respectively. All the CD spectra in this work were obtained by scanning from 190 to 260 nm in a MOS-450 spectrometer consisting of a quartz cuvettes of 1 mm optical path length at 25 °C. All the data were expressed in terms of mean residual ellipticity (h) in deg cm^2 $dmol^{-1}$.

Fabrication of the Proposed ECL Biosensor. After ultrasonic cleaning with ultrapure water and ethanol, bare GCE was successively polished using 0.3 and 0.05 μm Al_2O_3 powder to a mirror-like surface. Then, the cleaned GCE was immersed into 1% $HAuCl_4$ solution at −0.2 V for 30 s to deposit Au film (DpAu) on the surface. It should be noted that after each step below, the modified electrode was rinsed thoroughly with PBS (10 mmol/L, pH 7.4) to get rid of the unabsorbed species. First of all, GCE/DpAu was immersed into HWR (50 ng/mL) solution for 60 min to capture HWR via Au-S bond at 4 °C. After that, the electrode was dipped in 0.1% BSA solution at 37 °C for 1 h to block the non-specific binding sites of Ab_1. Then, the electrode was immersed into the Ab_1 solution (5 ug/mL) for 50 min to finish the incubation at 4 °C. Following that, 10 uL of PCT with different concentrations were incubated for 40 min at 37 °C. Finally, 10 uL of ABEI-Ft@Au-HWR-Ab_2 bioconjugate was covered on the obtained surface for sandwiched immunoreaction for at 37 °C. The biosensor was fully constructed and stored at 4 °C for following detection, and the fabrication process of the proposed biosensor was presented in **Scheme 1**.

Electrochemical and ECL Measurements. Cyclic voltammetry (CV) and MPI-F ECL analyzer were employed for the electrochemical and ECL measurements, respectively. A conventional three-electrode system containing the modified GCE as working electrode, a platinum wire as counter electrode and an Ag/AgCl electrode (saturated KCl) as reference electrode. The ECL detection was carried out in 10 mL of PBS (0.1 mol/L, pH 8.0) containing 30 mmol/L H_2O_2 at room temperature with parameters of photomultiplier tube voltage (800 V), scan voltage (from 0 to 0.58 V) and the scan rate (100 mV/s).

■ RESULTS AND DISCUSSION

Characterizations of ABEI-Ft@Au Nanostructure. The morphologies of pure ferritin and ABEI-Ft@Au were demonstrated by negative staining transmission electron microscopy (TEM) and high-resolution transmission electron microscopy (HRTEM). As shown in Figure 1A, pure ferritins with outer and inner diameter of ~12 nm and ~ 8 nm can be seen clearly. After sphere Au NPs with uniform size of 3.8 ± 0.2 nm were in situ synthesized on ABEI-Ft successfully (Figure 1B), the ABEI-Ft@Au were well-dispersed with no obvious aggregations. In Figure 1C, single ABEI-Ft@Au nanostructure was clearly presented, which was further characterized by atomic force microscope (AFM) topography. As shown in Figure 1D and E, the thickness of ABEI-Ft and Au NP were approximately 12.3 nm and 4.0 nm, respectively. Diameter distribution of Au NPs was shown Figure S1A. Besides, energy dispersive X-ray (EDX) showed C, N, O, P, S, Fe, Au signals, which was consistent with the elementary composition of ABEI-Ft@Au (Figure S1B). Then, the UV-vis absorption spectrum (Figure 1F) was further used to prove the synthesis of ABEI-Ft@Au. The absorption peak of ferritin was found at 280 nm, while the ABEI's were found at 226, 283 and 322 nm. Compared with ferritin and ABEI, the absorption peaks of ABEI-Ft at 226 nm and 322 nm faded away while the absorption peak at 280 nm became wider, which indicated the successful crosslinking of ABEI with ferritin. After the in situ growth of Au NPs, a new absorption peak was found at 519 nm compared with ABEI-Ft, indicating the successful preparation of ABEI-Ft@Au nanostructure.

Site-Oriented Capture of Antibody via HWR. HPLC was used to demonstrate the efficient combination of HWR with GCE/DpAu (**Supporting Information**, Figure S2A and B) and

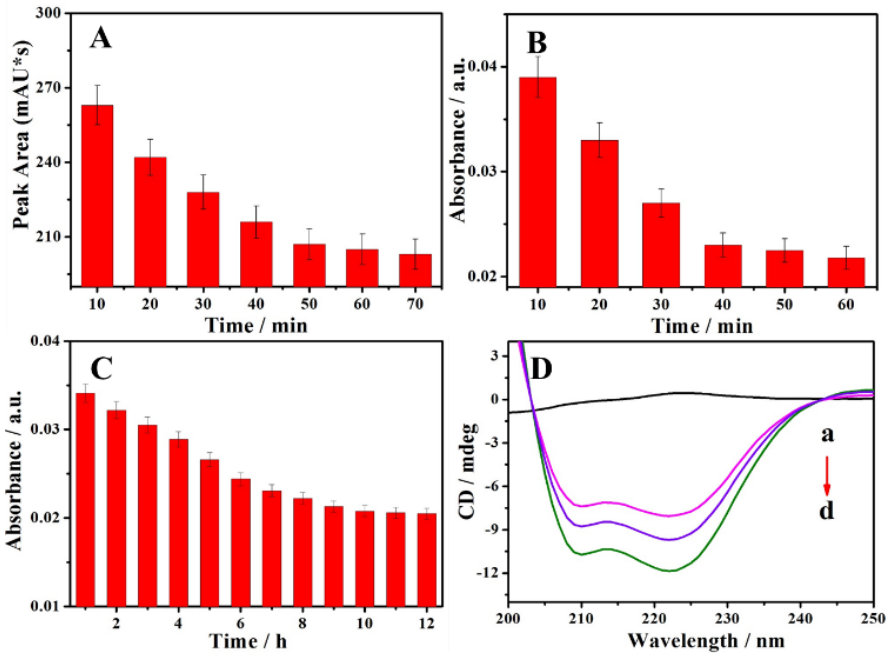

Figure 2. (A)HPLC results of uncoupled HWR (50 ng/mL) after coupling with ABEI-Ft@Au from 10 to 70 min. (B) UV-vis absorption of uncaptured Ab_2 by HWR in a time range from10 to 60 min. (C) UV-vis absorption spectrum of uncaptured Ab_2 by Au-N adsorption in a time range from 1 to 12 h. (D) CD spectra of pure HWR (a), ABEI-Ft@Au (b), ABEI-Ft@Au-Ab_2 (c), ABEI-Ft@Au-HWR-Ab_2 (d).

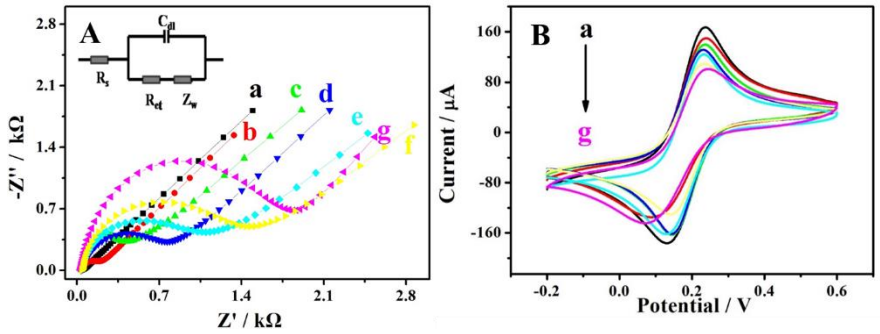

Figure 3. (A) EIS profiles of stepwise modified electrodes in 10 mL of PBS (pH 7.4, 0.1mol/L) containing 0.1mol/L KCl and mmol/L $[Fe(CN)_6]^{3-/4-}$: (a) GCE/DpAu, (b) bare GCE, (c) GCE/DpAu/HWR, (d) GCE/DpAu/HWR/BSA, (e) GCE/DpAu/HWR/BSA/Ab_1, (f) GCE/DpAu/HWR/BSA/Ab_1/PCT, (g) GCE/DpAu/HWR/BSA/Ab_1/PCT/ABEI-Ft@Au-HWR-Ab_2. (B) CV profiles of each step showed in (A).

ABEI-Ft@Au via Au-S bond. First of all, 1 mL of ABEI-Ft@Au solution were mixed with HWR solution (50 ng/mL) and coupled for different time at 4 °C. After centrifugation, the supernatants were tested and corresponding peak areas of HWR were recorded. As shown in Figure 2A, the curves levelled off at 50 min and kept constant. According to the Peak Area (P) = 162.1, the unconnected HWR amount was calculated to be about 31.62 ng using the regression equation P=32.8202 + 86.1905 ×lg c (R^2= 0.995) in Figure S2C, which indicated that approximately 18.45 ng of HWR (36.76%) were captured via Au-S bond in 50 min.

After coupling with HWR for 50 min, 1 mL of Ab_2 solution (5 ug/mL) was added and incubated for different time at 4 °C. The supernatants were collected for UV-vis absorption test. As shown in Figure 2B, the absorbance levelled off at 40 min and stayed constant. According to the absorbance (A) = 0.0231, the unconnected antibody amount was calculated to be about 2.44 ug using the regression equation A=0.00706×c + 0.00575 (R^2= 0.998) in Figure S2D, which indicated that 2.56 ug of Ab_2 were captured by HWR in 40 min.

As a comparison, ABEI-Ft@Au without HWR modification was directly mixed with 1 mL of Ab_2 solution (5 ug/mL) for different time at 4 °C. During the incubation process, antibody could connect with GCE/DpAu via Au-N adsorption. When the incubation time reached to 10 h (Figure 2C), corresponding absorbance of 0.023 was obtained, which was similar with the value of HWR method. It should be noted that this incubation time was 10 times longer than HWR method when incubating the same amount of antibody, which revealed the advance of using HWR as an antibody capturer for shortening incubation time of antibody.

The biological activity Ab_2 after HWR interaction and Au-N adsorption method was further demonstrated by CD spectra. As known, α-helix of secondary protein structure has specific absorption peaks at wavelength of 210 nm and 222 nm. Despite the incubated amount of Ab_2 was same by comparing their absorbance at 280 nm, the activity of Ab_2 can be different using site-oriented or random immobilizing method. As shown in Figure 2D, it can be inferred that the Ab_2 activity obtained by using HWR method was better maintained than that obtained by Au-N adsorption method, highlighting the advance of using HWR specific interaction to obtain a better maintained activity of Ab_2 than traditional Au-N adsorption.

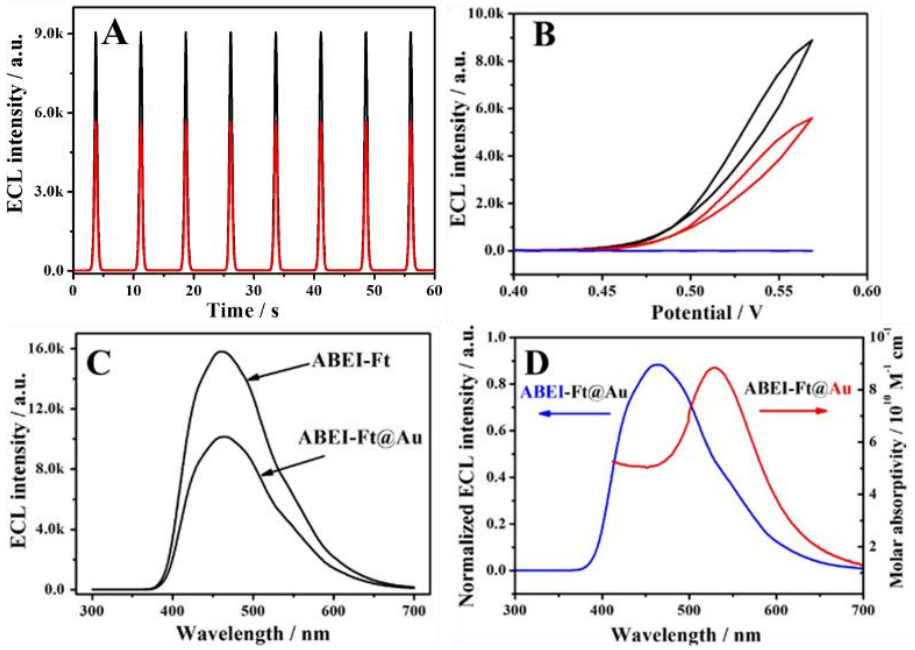

Figure 4. ECL-time curves (A) and ECL-potential curves (B) of bare GCE (blue curve), ABEI-Ft (black curve) and ABEI-ApoFt (red curve) in 10 mL of PBS (pH 8.0, 0.1 mol/L) contaning 30 mmol/L of H_2O_2. (C) ECL emission spectrum of ABEI-Ft (5 ug/mL) and ABEI-Ft@Au (5 ug/mL) in 10 mL of PBS (pH 8.0, 0.1 mol/L) contaning 30 mmol/L of H_2O_2. (D) Overlap between ECL emission spectrum (blue curve) and molar absorptivity spetrum (red curve) of ABEI-Ft@Au.

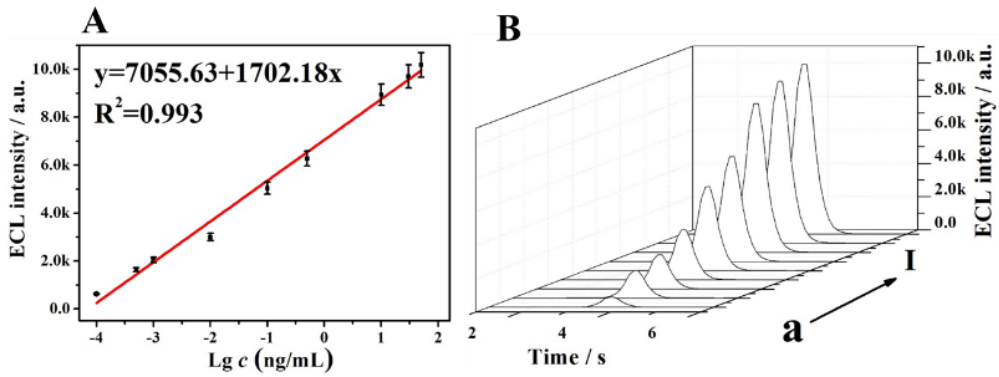

Figure 5. (A) calibration curve and corresponding ECL-time curve (B) of biosensor incubated with PCT of different concentrations: (a)100 fg /mL, (b) 500 fg/mL, (c) 1 pg/mL, (d) 10 pg/mL, (e) 100 pg/mL, (f) 500 pg/mL, (g) 10 ng/mL, (h) 30 ng/mL, (i) 50 ng/mL.

Electrochemical Characterizations of ECL Biosensor. Stepwise characterization of the proposed biosensor was confirmed with electrochemical impedance spectroscopy (EIS) and CV profiles conducted in $[Fe(CN)_6]^{4-/3-}$ (5 mmol/L) solution containing KCl (0.1 mol/L). Impedance spectra of GCE at different modified steps were shown in Figure 3A. GCE/DpAu (curve a) showed a smaller semicircle compared with bare GCE (curve b) because of the promotion of surface electron transmission by Au NPs. After the continuous modifications of nonconductive HWR, BSA, Ab_1 and PCT on the GCE surface, resistance (curve c, d, e and f) increased sequentially. After the final modification of ABEI-Ft@Au-HWR-Ab_2 bioconjugate (curve g), the resistance further increased. Simulation parameters of equivalent circuit components were shown in Table S1 and corresponding structural confirmations of this assembly process were shown in Figure S3. All the results above were consistent with the CV profiles in Figure 3B, indicating the superficial construction of the proposed ECL biosensor was successful.

Enhancement of ECL Emission by Ferric Nanocore. In order to demonstrate the enzyme-mimic activity of ferric nanocore, apoferritin (apoFt) was utilized to construct the ECL biosensor. ABEI-apoFt (5 ug/mL) and ABEI-Ft (5 ug/mL) were prepared. Under same experimental conditions, ECL signals of bare GCE, ABEI-apoFt and ABEI-Ft were recorded, respectively. As shown in Figure 4A and B, ECL signal generated by ABEI@Ft (curve a) was 1.6 times higher than ABEI@apoFt (curve b) while no ECL signals generated from bare GCE. Moreover, ECL responses of ABEI-Ft and ABEI-apoFt under different H_2O_2 concentrations were shown in Figure S4. The possible ECL enhancement mechanism was inferred as follows.[17, 18] In the anodic scanning process, after the deprotonation and chemical oxidation of ABEI, the radical anion of ABEI ($ABEI^{\bullet-}$) was generated (1). Then, ferric nanocore (FeOOH) facilitated the deposition of H_2O_2 to produce $OH^{\bullet}$ and $O_2^{\bullet-}$ (2). As oxidants, $OH^{\bullet}$ and $O_2^{\bullet-}$ reacted with $ABEI^{\bullet-}$ to form the excited state $(ABEI_{ox})^*$(3). In the final redox process (4), $(ABEI_{ox})^*$ decayed back to the ground state to finish the ECL emission process.

$$ABEI \xrightarrow[-2H^+]{-e^-} ABEI^{\bullet-} \quad (1)$$

$$H_2O_2 \xrightarrow{FeOOH} OH^{\bullet} + O_2^{\bullet-} \quad (2)$$

$$ABEI^{\bullet-} + OH^{\bullet}/O_2^{\bullet-} \longrightarrow (ABEI_{ox})^* + products \quad (3)$$

$$(ABEI_{ox})^* \longrightarrow ABEI_{ox} + h\nu \quad (4)$$

ECL Quenching Mechanism Discussion. As shown in Figure 4C, the ECL emission of ABEI-Ft@Au decreased from 1,5804 a.u. to 6954 a.u., indicating that the efficiency of 56 % in the energy transfer process and the consistency study of quenching efficiency was shown in Figure S5 and Table S2. In order to rationalize the quenching mechanism, possible FRET and NSET mechanism were discussed, respectively. Since the UV-vis absorption spectra of ABEI-Ft@Au significantly overlapped with its ECL spectrum from 400 to 700 nm (Figure 4D) and the distance between Au NPs and proximal ABEI was assumed to be less than 10 nm, thus FRET theory was firstly applied to demonstrate the quenching process. According to previous works, the Förster radius R_0 was calculated to be 13.84 nm (detailed calculation was in **Supporting Information**). In Persson and Lang's model,[11] d is the distance from the nanosurface of Au NPs to the proximal ABEI, d_0 stands for the separation distance when the energy-transfer efficiency is 50 %. Therefore, the radius d_0 can be calculated by:

$$d_0 = \left(\frac{0.225\Phi_D c^3}{\omega_D^2 \omega_F k_F}\right)^{1/4}$$

where Φ_D (quantum yield of ABEI) = 0.043, c (velocity of light) =3× 10^8 m/s, ω_D (angular frequency of ABEI) = 4.07 × 10^{15} rad/s, ω_F (Fermi frequency of Au) = 8.3 × 10^{15} rad/s, and k_F (Fermi wave vector) = 1.2 × 10^{10}/m. Therefore, the d_0 value was calculated to be 3.54 nm using the above data. Based on the estimated values of R_0 and d_0, the energy transfer efficiency correlated with the following equation:

$$\Phi_{ET} = \frac{1}{1 + \left(\frac{d}{d_0}\right)^4}$$

where Φ_{ET} is the energy-transfer efficiency, d is the separation distance between Au NPs and proximal ABEI, n is the power that owns a value of 6 for the FRET($r_0 = R_0$) or 4 for the NSET ($r_0 = d_0$), respectively.[13] When the Φ_{ET} was 56%, the estimated separation distance between Au NPs and proximal ABEI based on FRET and NSET mechanism were calculated to be 13.29 nm and 3.33 nm, respectively. However, it should be highlighted that in a qualified ECL quenching system based on FRET theory, the Förster distance R_0 value should be in the range of 2 - 6 nm and the distance should be no longer than 10 nm.[15, 35] Thus, it can be concluded that NSET theory is the dominant energy-transfer mechanism for the proposed ECL quenching system. Correlation between experimentally obtained quenching efficiency with the NSET theoretical plots of the quenching efficiency against the separation distance was shown in Figure S7, from which the distance between ABEI and proximal Au NP was estimated to be 3.33 nm in one donor-acceptor nanostructure when the energy transfer efficiency was 56%.

Table 1. Comparison of Proposed Method with Other Reported Methods for PCT Detection.

Methods	Linear range (ng/mL)	Detection limit (pg/mL)	Ref
fluorescence	0.1 —10	0.25	36
surface plasmon resonance	20 — 4000	9.9	37
electrochemical	0.0018 — 500	0.36	38
electrochemical	0.01 —100	1.23	39
electrochemical	0.01 — 350	0.5	40
ECL	0.01 —20	3.4	41
ECL	0.0001 — 50	0.041	this work

ECL Responses of Biosensor Toward PCT. Under the optimized experimental conditions (**Supporting information,** Figure S6**)**, different concentrations of PCT were detected by the proposed ECL biosensor. The relationship between ECL intensity (I_{ECL}) and logarithm of PCT concentration (lg c) was presented in Figure 5A where the linear relation of I_{ECL} =1702.18 lg c +7055.63 with a correlation coefficient of 0.993 was displayed. Corresponding ECL intensity-potential curves were presented in Figure 5B. This established ECL biosensor exhibited a wide linear range of 0.0001 - 50 ng/mL, and the detection limit of 0.041 pg/mL (S/N=3) was lower than other previous works listed in Table 1, [36-41] highlighting the advance of this ECL-NSET strategy for PCT detection.

Analysis of PCT in Human Serum. SIRS caused by a bacterial, viral, or fungal infection has become a primary cause of patients death although new generation of antibiotics, chemical therapies or other medical advances have all been utilized to try to prevent it. PCT as a typical biomarker of SIRS in human serum plays a crucial role in realizing the accurate and reliable diagnostics in the early stage of SIRS. The PCT concentration in human serum specimens obtained from local hospital was detected to be 3.28 ng/mL using the proposed biosensor. In order to investigate the accuracy and reliability of the obtained result, standard addition method was applied. The serum samples were divided into four groups and each group was spiked with 0.1 ng/mL, 3 ng/mL, 5 ng/mL, 10 ng/mL of PCT standard samples, respectively. As shown in Table S3, the recovery values were acceptable with RSD (between 0.91% and 3.58%, n=5), proving the application potential of the proposed biosensor in detecting PCT concentration in human serum samples.

■CONSLUSIONS

In summary, an ultrasensitive ECL biosensor based on a highly efficient ECL-NSET donor-acceptor nanostructure of ABEI-Ft@Au was developed. The excitation energy transfer mechanism between ABEI and Au NPs was firstly demonstrated to follow the NSET theory instead of FRET theory. Besides, HWR as specific Fc portion capturer was firstly employed to realize site-oriented antibody capturing, which not only facilitated the incubation process of antibody on carriers, but also helped maintain its biological activity to a larger extent to improve sensitivity of biosensor. Using PCT as a target, the proposed ECL biosensor exhibited sensitive response to PCT concentration with wide linear range and low detection limit in human serum detection, indicating its potential application in biomarkers detection. We believe that the established ECL-NSET system can inspire deeper and informative studies in nanometal-based ECL quenching mechanism and developments of peptides ligands in realizing site-oriented immobilization of antibody in bioanalysis.

■ ASSOCIATED CONTENT

Supporting Information

Materials and reagents, apparatus, preparation of apoferritin, diameter distribution of Au NPs, EDX spectrum of ABEI-Ft@Au, site-oriented immobilization of Ab_1 via HWR, simulation parameters of equivalent circuit components, ECL responses of ABEI-Ft and ABEI-apoFt under different H_2O_2 concentrations, consistency study of quenching efficiency under different H_2O_2 concentrations, optimization of H_2O_2 concentration and pH values of PBS, specificity, stability and reproducibility of biosensor, NSET theoretical plots of the quenching efficiency against the separation distance, FRET theory study and recovery results of PCT in real samples.

■ AUTHOR INFORMATION

Corresponding Author

*E-mail: sdjndxwq@163.com (Q. Wei)

ORCID

Qin Wei: 0000-0002-3034-8046

Notes

The authors declare no competing financial interest.

■ ACKNOWLEDGMENTS

This work was supported by the National Key Scientific Instrument and Equipment Development Project of China (No.21627809); National Natural Science Foundation of China (No.21575050, 21505051, 21777056, 21427808).

■ REFERENCES

(1) Yang, L.; Zhu, W. J.; Ren, X.; Khan, M. S.; Zhang, Y.; Du, B.; Wei, Q., Macroporous Graphene Capped Fe_3O_4 for Amplified Electrochemiluminescence Immunosensing of Carcinoembryonic Antigen Detection Based on CeO_2@TiO_2. *Biosens. Bioelectron.* 2017, *91*, 842-848.

(2) Yang, L.; Li, Y. Y.; Zhang, Y.; Fan, D. W.; Pang, X. H.; Wei, Q.; Du, B., 3D Nanostructured Palladium-Functionalized Graphene-Aerogel-Supported Fe_3O_4 for Enhanced $Ru(bpy)_3^{2+}$-Based Electrochemiluminescent Immunosensing of Prostate Specific Antigen. *ACS Appl. Mater. Interfaces.* 2017, *9* (40), 35260-35267.

(3) Xing, B.; Zhu, W. J.; Zheng, X. P.; Zhu, Y. Y.; Wei, Q.; Wu, D., Electrochemiluminescence Immunosensor Based on Quenching Effect of SiO_2@PDA on SnO_2/rGO/Au NPs-luminol for Insulin Detection. *Sens. Actuator, B* 2018, *265*, 403-411.

(4) Zhou, Y.; Yu, Y.; Chai, Y.; Yuan, R., Electrochemical Synthesis of Silver Nanoclusters on Electrochemiluminescent Resonance Energy Transfer Amplification Platform for Apo-A1 Detection. *Talanta.* 2018, *181*, 32-37.

(5) Chen, M. M.; Wang, Y.; Cheng, S. B.; Wen, W.; Zhang, X.; Wang, S.; Huang, W. H., Construction of Highly Efficient Resonance Energy Transfer Platform Inside a Nanosphere for Ultrasensitive Electrochemiluminescence Detection. *Anal. Chem.* 2018, *90* (8), 5075-5081.

(6) Chen, X.; Gui, W.; Ma, Q., Ultrasensitive Detection of EGFR Gene Based on Surface Plasmon Resonance Enhanced Electrochemiluminescence of CuZnInS Quantum Dots. *Anal. Chim. Acta.* 2018, *1009*, 73-80.

(7) Wu, M. S.; He, L. J.; Xu, J. J.; Chen, H. Y., RuSi@$Ru(bpy)_3^{2+}$/Au@Ag_2S Nanoparticles Electrochemiluminescence Resonance Energy Transfer System for Sensitive DNA Detection. *Anal. Chem.* 2014, *86* (9), 4559-4565.

(8) Ding, S. H.; Gao, B. H.; Shan, D.; Sun, Y. M.; Cosnier, S., TiO_2 Nanocrystals Eelectrochemiluminescence Quenching by Biological Enlarged Nanogold Particles And Its Application for Biosensing. *Biosens. Bioelectron*. 2012, *39* (1), 342-345.

(9) Lu, Q.; Wei, W.; Zhu, Z. X.; Zhou, Z. X.; Zhang, Y. J.; Liu, S. Q., Electrochemiluminescence Resonance Energy Transfer Between Graphene Quantum Dots And Gold Nanoparticles for DNA Damage Detection. *Analyst*. 2014, *139* (10), 2404-2410.

(10) Lu, H.; Pan, J.; Wang, Y.; Ji, S. Y.; Chen, H. Y., Electrochemiluminescence Energy Resonance Transfer System between RuSi Nanoparticles and Hollow Au Nanocages for Nucleic Acid Detection. *Anal. Chem.* 2018, *90* (17), 10434-10441

(11) Jennings, T. L.; Singh, M. P.; Strouse, G. F., Fluorescent Lifetime Quenching Near d = 1.5 nm Gold Nanoparticles: Probing NSET Validity. *J. Am. Chem. Soc.* 2006, *128* (16), 5462-5467.

(12) Yun, C. S.; Javier, A.; Jennings, T.; Fisher, M.; Hira, S.; Peterson, S.; Hopkins, B.; Reich, N. O.; Strouse, G. F., Nanometal Surface Energy Transfer in Optical Rulers, Breaking the FRET Barrier. *J. Am. Chem. Soc.* 2005, *127* (9), 3115-3119.

(13) Prajapati, R.; Chatterjee, S.; Bhattacharya, A.; Mukherjee, T. K., Surfactant-Induced Modulation of Nanometal Surface Energy Transfer from Silicon Quantum Dots to Silver Nanoparticles. *J. Phys. Chem. C.* 2015, *119* (23), 13325-13334.

(14) Li, Y.; Li, P.; Zhu, R.; Luo, C.; Li, H.; Hu, S.; Nie, Z.; Huang, Y.; Yao, S., Multifunctional Gold Nanoclusters-Based Nanosurface Energy Transfer Probe for Real-Time Monitoring of Cell Apoptosis and Self-Evaluating of Pro-Apoptotic Theranostics. *Anal. Chem.* 2016, *88* (22), 11184-11192.

(15) Sarkar, P. K.; Polley, N.; Chakrabarti, S.; Lemmens, P.; Pal, S. K., Nanosurface Energy Transfer Based Highly Selective and Ultrasensitive "Turn on" Fluorescence Mercury Sensor. *ACS Sensors.* 2016, *1* (6), 789-797.

(16) Chen, C.; Midelet, C.; Bhuckory, S.; Hildebrandt, N.; Werts, M. H. V., Nanosurface Energy Transfer from Long-Lifetime Terbium Donors to Gold Nanoparticles. *J. Phys. Chem. C.* 2018, *122* (30), 17566-17574.

(17) Liu, Y.; Wang, H.; Xiong, C.; Yuan, Y.; Chai, Y.; Yuan, R., A Sensitive Electrochemiluminescence Immunosensor Based on Luminophore Capped Pd@Au Core-Shell Nanoparticles as Signal Tracers and Ferrocenyl Compounds as Signal Enhancers. *Biosens. Bioelectron.* 2016, *81*, 334-340.

(18) Yang, H. Y.; Wang, H. J.; Xiong, C. Y.; Chai, Y. Q.; Yuan, R., Intramolecular Self-Enhanced Nanochains Functionalized by an Electrochemiluminescence Reagent and Its Immunosensing Application for the Detection of Urinary beta2-Microglobulin. *ACS Appl. Mater. Interfaces.* 2017, *9* (41), 36239-36246.

(19) Wang, H.; Yuan, Y.; Zhuo, Y.; Chai, Y.; Yuan, R., Sensitive Electrochemiluminescence Immunosensor for Detection of N-Acetyl-beta-d-glucosaminidase Based on a "Light-Switch" Molecule Combined with DNA Dendrimer. *Anal. Chem.* 2016, *88* (11), 5797-5803.

(20) Günther, J.; Patrick, van R.; Barbara, S. M.; Alexander, B.; Ferritin: A Versatile Building Block for Bionanotechnology. *Chem. Rev.*, **2015**, *115* (4), 1653-1701.

(21) Liu, G.; Wu, H.; Wang, J.; Lin, Y., Apoferritin-Templated Synthesis of Metal Phosphate Nanoparticle Labels for Electrochemical Immunoassay. *Small.* **2006,** *2* (10), 1139-1143.

(22) Dostalova, S.; Cerna, T.; Hynek, D.; Koudelkova, Z.; Vaculovic, T.; Kopel, P.; Hrabeta, J.; Heger, Z.; Vaculovicova, M.; Eckschlager, T.; Stiborova, M.; Adam, V., Site-Directed Conjugation of Antibodies to Apoferritin Nanocarrier for Targeted Drug Delivery to Prostate Cancer Cells. *ACS Appl. Mater. Interfaces.* **2016,** *8* (23), 14430-14441.

(23) Peng, S.; Kim, J. H.; Park, S. J., Size controlled preparation of CdTe nanoparticles by apoferritin. *J. Cryst.Growth.* **2017,** *468*, 79-83.

(24) Elmas, S. N. K.; Guzel, R.; Say, M. G.; Ersoz, A.; Say, R., Ferritin Based Bionanocages as Novel Biomemory Device Concept. *Biosens. Bioelectron.* **2018,** *103*, 19-25.

(25) Espinosa, A.; Curcio, A.; Cabana, S.; Radtke, G.; Bugnet, M.; Kolosnjaj-Tabi, J.; Pechoux, C.; Alvarez-Lorenzo, C.; Botton, G. A.; Silva, A. K. A.; Abou-Hassan, A.; Wilhelm, C., Intracellular Biodegradation of Ag Nanoparticles, Storage in Ferritin, and Protection by a Au Shell for Enhanced Photothermal Therapy. *ACS Nano.* **2018,** *12* (7), 6523-6535.

(26) Shuvaev, V. V.; Khoshnejad, M.; Pulsipher, K. W.; Kiseleva, R. Y.; Arguiri, E.; Cheung-Lau, J. C.; LeFort, K. M.; Christofidou-Solomidou, M.; Stan, R. V.; Dmochowski, I. J.; Muzykantov, V. R., Spatially Controlled Assembly of Affinity Ligand and Enzyme Cargo Enables Targeting Ferritin Nanocarriers to Caveolae. *Biomaterials.* **2018,** *185*, 348-359.

(27) Wu, D.; Wei, Y.; Ren, X.; Ji, X.; Liu, Y.; Guo, X.; Liu, Z.; Asiri, A. M.; Wei, Q.; Sun, X., $Co(OH)_2$ Nanoparticle-Encapsulating Conductive Nanowires Array: Room-Temperature Electrochemical Preparation for High-Performance Water Oxidation Electrocatalysis. *Adv. Mater.* **2018,** *30* (9), 1705366-1705372.

(28) Tang, Z.; Wu, H.; Zhang, Y.; Li, Z.; Lin, Y., Enzyme-Mimic Activity of Ferric Nano-Core Residing in Ferritin and Its Biosensing Applications. *Anal. Chem.* **2011,** *83* (22), 8611-8616.

(29) Makaraviciute, A.; Ramanaviciene, A., Site-Directed Antibody Immobilization Techniques for Immunosensors. *Biosens. Bioelectron.* **2013,** *50*, 460-471.

(30) Liu, F.; Wang, L.; Wang, H.; Yuan, L.; Li, J.; Brash, J. L.; Chen, H., Modulating the Activity of Protein Conjugated to Gold Nanoparticles by Site-Directed Orientation and Surface Density of Bound Protein. *ACS Appl. Mater. Interfaces.* **2015,** *7* (6), 3717-3724.

(31) Yang, H.; Gurgel, P. V.; Williams, D. K., Jr.; Bobay, B. G.; Cavanagh, J.; Muddiman, D. C.; Carbonell, R. G., Binding site on human immunoglobulin G for the affinity ligand HWRGWV. *J. Mol. Recognit.* **2010,** *23* (3), 271-282.
(32) Lim, J. M.; Ryu, M. Y.; Kim, J. H.; Cho, C. H.; Park, T. J.; Park, J. P., An Electrochemical Biosensor for Detection of the Sepsis-Related Biomarker Procalcitonin. *RSC Adv.* **2017,** *7* (58), 36562-36565.
(33) Liu, F.; Xiang, G.; Chen, X.; Luo, F.; Jiang, D.; Huang, S.; Li, Y.; Pu, X., A Novel Strategy of Procalcitonin Detection Based on Multi-Nanomaterials of Single-Walled Carbon Nanohorns-Hollow Pt Nanospheres/PAMAM as Signal Tags. *RSC Adv*. 2014, *4*, 13934-13940.
(34) Ianeselli, A.; Orioli, S.; Spagnolli, G.; Faccioli, P.; Cupellini, L.; Jurinovich, S.; Mennucci, B., The Atomic Detail of Protein Folding Revealed by an Ab Initio Reappraisal of Circular Dichroism. *J. Am. Chem. Soc.* 2018, *140* (10), 3674-3682 .
(35) Mandal, S.; Ghatak, C.; Rao, V. G.; Ghosh, S.; Sarkar, N., Pluronic Micellar Aggregates Loaded with Gold Nanoparticles (Au NPs) and Fluorescent Dyes: A Study of Controlled Nanometal Surface Energy Transfer. *J. Phys. Chem. C*, 2012, *116* (9), 5585-5597.
(36) Zhou, Y.; Shao, X. M.; Han, Y. W.; Zhang, H.M., Detection of Procalcitonin (PCT) Using the Double Antibody Sandwich Method Based on Fluorescence Resonant Energy Transfer Between Upconversion Nanoparticles and Quantum Dots. *Anal. Methods*. 2018, 10, 1015-1022.
(37) Gulsu, S.; Erdogan, O.; Abbas Yousefi, R.; Lokman, U.; Ridvan, S.; Adil, D., Rapid Real-Time Detection of Procalcitonin Uing a Microcontact Imprinted Surface Plasmon Resonance Biosensor. *Analyst.* **2013,** *138* (21), 6422-6428.
(38)Shen, W. J.; Zhuo, Y.; Chai, Y. Q.; Yang, Z. H.; Han, J.; Yuan, R., Enzyme-Free Electrochemical Immunosensor Based on Host-Guest Nanonets Catalyzing Amplification for Procalcitonin Detection. *ACS Appl. Mater. Interfaces.* **2015,** *7* (7), 4127-4134.
(39) Yang, Z. H.; Zhuo, Y.; Yuan, R.; Chai, Y. Q., Electrochemical Activity And Electrocatalytic Property of Cobalt Phthalocyanine Nanoparticles-Based Immunosensor for Sensitive Detection of Procalcitonin. *Sens. Actuator, B* **2016,** *227*, 212-219.
(40) Fang, Y. S.; Wang, H. Y.; Wang, L. S.; Wang, J. F.; Electrochemical Immunoassay for Procalcitonin Antigen Detection Based on Signal Amplification Strategy of Multiple Nanocomposites. *Biosens. Bioelectron.* **2014,** *51* (1), 310-316.
(41) Li, H. N.; Sun, Y. Y.; Elseviers, J.; Muyldermans, S.; Liu, S. Q.; Wan, Y. K., A Nanobody-Based Electrochemiluminescent Immunosensor for Sensitive Detection of Human Procalcitonin. *Analyst.* **2014,** *139* (15), 3718-3721.

For TOC graphic only